METABOLISM

Lactation improves pancreatic β cell mass and function through serotonin production

Joon Ho Moon[1,2]*, Hyeongseok Kim[1,3]*, Hyunki Kim[1], Jungsun Park[1], Wonsuk Choi[1], Wongun Choi[1], Hyun Jung Hong[4], Hyun-Joo Ro[5,6], Sangmi Jun[5,6], Sung Hee Choi[2], Ronadip R. Banerjee[7], Minho Shong[4], Nam Han Cho[8], Seung K. Kim[9], Michael S. German[10†], Hak Chul Jang[2†], Hail Kim[1†]

Pregnancy imposes a substantial metabolic burden on women through weight gain and insulin resistance. Lactation reduces the risk of maternal postpartum diabetes, but the mechanisms underlying this benefit are unknown. Here, we identified long-term beneficial effects of lactation on β cell function, which last for years after the cessation of lactation. We analyzed metabolic phenotypes including β cell characteristics in lactating and non-lactating humans and mice. Lactating and non-lactating women showed comparable glucose tolerance at 2 months after delivery, but after a mean of 3.6 years, glucose tolerance in lactated women had improved compared to non-lactated women. In humans, the disposition index, a measure of insulin secretory function of β cells considering the degree of insulin sensitivity, was higher in lactated women at 3.6 years after delivery. In mice, lactation improved glucose tolerance and increased β cell mass at 3 weeks after delivery. Amelioration of glucose tolerance and insulin secretion were maintained up to 4 months after delivery in lactated mice. During lactation, prolactin induced serotonin production in β cells. Secreted serotonin stimulated β cell proliferation through serotonin receptor 2B in an autocrine and paracrine manner. In addition, intracellular serotonin acted as an antioxidant to mitigate oxidative stress and improved β cell survival. Together, our results suggest that serotonin mediates the long-term beneficial effects of lactation on female metabolic health by increasing β cell proliferation and reducing oxidative stress in β cells.

INTRODUCTION

Pregnancy imposes a substantial metabolic burden on women through weight gain and increased insulin resistance. Accordingly, women have an increased risk of diabetes after repeated deliveries (*1*, *2*). Various factors, including a history of gestational diabetes, maternal age, and obesity, affect women's risk of progressing to diabetes (*3*–*6*). Among these factors, lactation has been reported to reduce the risk of maternal postpartum diabetes in a dose-dependent manner. Parous women who did not lactate have an increased risk of diabetes compared to nulliparous women, but lactation for more than 3 months appears to reduce this risk comparable to nulliparous women (*7*). Epidemiological studies have shown that this beneficial effect of lactation in preventing postpartum diabetes can last up to 30 years after delivery (*8*, *9*). Lactation increases energy consumption (~500 kcal/day) and improves insulin sensitivity, but the mechanisms underlying the long-term beneficial effects of lactation have not been elucidated (*10*–*12*).

Serotonin [5-hydroxytryptamine (5-HT)] is synthesized from tryptophan by the sequential actions of tryptophan hydroxylase (TPH) and aromatic amino acid decarboxylase (AADC). 5-HT is present in peripheral tissues as well as in neuronal tissues (*13*), and it plays various roles in the heart (*14*), liver (*15*, *16*), adipose tissue (*17*, *18*), and bone (*19*). 5-HT exerts its biological action by binding to 5-HT receptor (HTR). In pancreatic β cells, 5-HT plays pivotal roles in compensating for physiological insulin resistance during pregnancy. Placental lactogen induces robust 5-HT production in β cells, and 5-HT, in turn, enhances β cell proliferation and insulin secretion through HTR2B and HTR3, respectively (*20*, *21*). 5-HT also plays an important role in regulating the adult β cell mass by stimulating β cell proliferation during the perinatal period (*22*).

During lactation, plasma prolactin concentration is increased, which may be able to induce 5-HT production in β cells and improve insulin secretory function (*20*, *23*, *24*). Thus, improved β cell function could be a possible mechanism for the long-term beneficial effects of lactation in women. In this study, we show that lactation improves glucose tolerance and insulin secretory function in humans. We also show that lactation improves β cell mass and insulin secretory function through 5-HT production in mice. Using mouse models, we show that prolactin induces 5-HT production in β cells through the sequential activation of prolactin receptor (PRLR) and signal transducer and activator of transcription 5 (STAT5), which, in turn, induces *Tph1* expression. 5-HT further activates HTR2B signaling to activate β cell proliferation during lactation. In addition, 5-HT derivatives act as direct antioxidants to enhance β cell survival upon oxidative stress.

RESULTS

Lactation improves glucose homeostasis and β cell function

To investigate whether lactation can improve glucose homeostasis and/or β cell function in postpartum women, women with a history of

[1]Graduate School of Medical Science and Engineering, Korea Advanced Institute of Science and Technology, Daejeon 34141, Korea. [2]Department of Internal Medicine, Seoul National University College of Medicine, Seoul 03080, Korea. [3]Department of Biochemistry, College of Medicine, Chungnam National University, Daejeon 35015, Korea. [4]Research Center for Endocrine and Metabolic Diseases, Chungnam National University School of Medicine, Daejeon 35015, Korea. [5]Center for Research Equipment, Korea Basic Science Institute, Cheongju 28119, Korea. [6]Center for Convergent Research of Emerging Virus Infection, Korea Research Institute of Chemical Technology, Daejeon 34114, Korea. [7]Division of Endocrinology, Diabetes and Metabolism, Department of Medicine, University of Alabama School of Medicine, Birmingham, AL 35294, USA. [8]Department of Preventive Medicine, Ajou University School of Medicine, Suwon 16499, Korea. [9]Department of Developmental Biology and Stanford Diabetes Research Center, Stanford University School of Medicine, Stanford, CA 94305, USA. [10]Diabetes Center, Hormone Research Institute and Department of Medicine, University of California San Francisco, San Francisco, CA 94143, USA.
*These authors contributed equally to this work.
†Corresponding author. Email: hailkim@kaist.edu (Hail Kim); janghak@snu.ac.kr (H.C.J.); michael.german@ucsf.edu (M.S.G.)

gestational diabetes or gestational impaired glucose tolerance (GIGT) were examined with the 75-g oral glucose tolerance test (OGTT) at 2 months postpartum and annually thereafter. A total of 174 women (lactated, $n = 85$; non-lactated, $n = 99$) were included in this analysis. Baseline characteristics, including age, body mass index, HbA1c concentration at diagnosis, and parity, were comparable between the lactating and non-lactating women (table S1). The initial follow-up at 2 months postpartum showed comparable glucose concentrations except for lower fasting glucose in lactating women compared to non-lactating women (Fig. 1A). At a mean of 3.6 years after delivery, women who had lactated maintained comparable glucose concentrations to 2 months postpartum, whereas the glucose tolerance deteriorated in women who had not lactated (Fig. 1B). The insulinogenic index was comparable between the two groups at the initial and last follow-up, whereas the Matsuda index was significantly higher in lactating and lactated women compared to their non-lactating counterparts ($P = 0.015$ and $P < 0.001$ for the initial and last follow-up, respectively) (Fig. 1C, Table 1, and table S2). The disposition index, a composite insulin secretory function of β cell considering the degree of insulin sensitivity, was significantly increased in lactated women at the last follow-up ($P = 0.020$) (Table 1). Insulin resistance is known to induce a compensatory increase of β cell mass and function (*25*, *26*). However, β cell function improved more in lactated women than in non-lactated women, although lactated women showed better insulin sensitivity than non-lactated women (Fig. 1C). These data suggest that the improved glucose tolerance in lactated women could be attributed to their improvement in β cell function regardless of insulin resistance.

To understand the physiology underlying the beneficial effect of lactation on β cell function, we established a mouse model for lactation and investigated whether this model could mimic the phenotypes observed in humans (Fig. 2A). Nine-week-old female mice were mated to give birth, and pups were either left with the mother (lactating) or removed from the cage (non-lactating) on the day of delivery. Lactation was stopped at 3 weeks postpartum by removing the pups from the cage. Both lactating and non-lactating mice were assessed at 3 weeks postpartum, and lactated and non-lactated mice were assessed at 6 weeks postpartum unless otherwise indicated.

Lactating mice gained more weight, but their glucose tolerance and insulin tolerance were improved (Fig. 2, B to D). The fasting insulin concentrations were lower in the lactating mice, but their glucose-stimulated insulin secretion was prominent at 15 min after glucose administration (Fig. 2E). Lactating mice thus exhibited an improved insulinogenic index (0 to 15 min), suggesting that their insulin secretory function was improved (fig. S1A). In lactated mice, the glucose tolerance remained improved but the insulin tolerance became comparable to that in non-lactated mice (Fig. 2, F and G). Glucose-stimulated insulin secretion was potentiated in lactated mice (Fig. 2H and fig. S1B). Improved glucose tolerance and insulin secretion were sustained in lactated mice up until 12 weeks postpartum and in lactated mice that had undergone repeated deliveries (fig. S1, C to H). Together, both glucose tolerance and β cell function were improved in lactated mice, and our mouse models mimicked the human phenotypes. These data also suggest that the long-term metabolic benefit of lactation can be attributed to the sustained improvement in β cell function.

To elucidate the mechanism underlying the beneficial effects of lactation on β cell function, we investigated the β cell mass and insulin secretory function in lactating and non-lactating mice. Lactating mice had larger pancreata than non-lactating mice, but no difference in pancreas weight was observed between lactated mice and non-lactated mice (fig. S2, A to D). In lactating mice, β cell mass was increased, although the insulin sensitivity was improved (Fig. 2, D and I). This increase in β cell mass was sustained after the cessation of lactation (Fig. 2J and fig. S2, E and F). The increase in β cell mass was mainly attributed to increased β cell proliferation during lactation but not to decreased β cell death after delivery (Fig. 2, K and L, and fig. S2, G to L). The insulin secretory function of isolated islets was not altered in lactating mice and lactated mice at 3 and 6 weeks postpartum or after repeated deliveries (fig. S3, A to C). However, insulin secretion from isolated islets became more prominent at 12 weeks postpartum, suggesting the potential benefit of lactation on insulin secretory function (fig. S3D). Together, these data indicate that increased β cell mass due to increased β cell proliferation during lactation can contribute to the long-term beneficial effects of lactation.

5-HT induces β cell proliferation and improves β cell function during lactation

During pregnancy, placental lactogen stimulates 5-HT production in β cells through the PRLR-STAT5-TPH1 cascade (*20*, *27*). Therefore, we hypothesized that prolactin induces 5-HT production in β cells during lactation through the PRLR-STAT5-TPH1 cascade. As

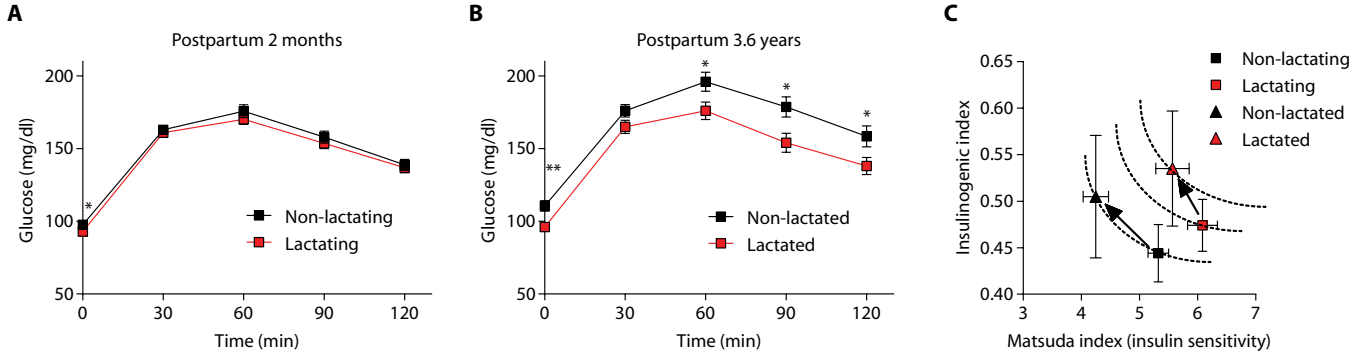

Fig. 1. Lactation improves glucose homeostasis and β cell function in postpartum women. (**A** to **C**) Metabolic phenotypes in postpartum women by lactation status. A total of 174 women (lactated, $n = 85$; non-lactated, $n = 99$) were included in the analysis. (A and B) Plasma glucose concentrations were measured during the 75-g OGTT (A) at 2 months postpartum in lactating and non-lactating women and (B) at a mean of 3.6 years after delivery in previously lactated and non-lactated women. (C) Hyperbolic curves plotting the Matsuda index (insulin sensitivity) and insulinogenic index during and after lactation. Data are means ± SEM. $^*P < 0.05$, $^{**}P < 0.01$, and $^{***}P < 0.001$.

Table 1. Lactation improves insulin sensitivity and β cell function in postpartum women. The Matsuda index, insulinogenic index, and disposition index during and after lactation (at 2 months postpartum in lactating/non-lactating women and at a mean of 3.6 years after delivery in lactated/non-lactated women). A total of 174 women (lactated, $n = 85$; non-lactated, $n = 99$) were included in the analysis. Data are expressed as the means and SEM. $^{*}P < 0.05$, $^{**}P < 0.01$, and $^{***}P < 0.001$.

	Initial follow-up					Last follow-up				
	Non-lactating	SEM	Lactating	SEM	*P*	Non-lactated	SEM	Lactated	SEM	*P*
Matsuda index (insulin sensitivity)	5.324	0.177	6.085	0.257	0.015*	4.249	0.218	5.569	0.287	0.000***
Insulinogenic index	0.444	0.031	0.474	0.028	0.500	0.505	0.066	0.535	0.062	0.230
Disposition index	2.229	0.163	2.642	0.170	0.087	2.212	0.261	3.108	0.498	0.020*

expected, plasma prolactin concentration was increased during lactation (Fig. 3A). The mRNA transcriptions of *Prlr* and *Tph1* were increased in pancreatic islets during lactation (Fig. 3, B and C), and prolactin induced *Tph1* mRNA expression in mouse β cell lines βTC3 and MIN6 (Fig. 3D). Immunofluorescence staining for 5-HT revealed robust 5-HT production in pancreatic β cells during lactation (Fig. 3E). Intracellular 5-HT concentration was ~200-fold higher in lactating islets compared to non-lactating islets (Fig. 3F). To further evaluate our hypothesis, we generated inducible β cell–specific *Prlr* knockout (*Prlr* βiKO) mice and *Tph1* KO (*Tph1* βiKO) mice, and induced KO by administering tamoxifen on the day of delivery in lactating control and KO mice (fig. S4, A to F). 5-HT was undetectable by immunofluorescence staining in the islets of lactating *Prlr* βiKO and *Tph1* βiKO mice (Fig. 3E). Thus, similar to pregnancy, prolactin induced 5-HT production in β cells during lactation via the PRLR-STAT5-TPH1 axis.

We further analyzed *Tph1* βiKO mice to investigate whether 5-HT production is necessary for the improvement of metabolic phenotypes seen during lactation. Glucose tolerance and insulin secretion were impaired in lactating *Tph1* βiKO mice (Fig. 3, G and H), despite similar insulin sensitivity at 3 weeks postpartum (fig. S5A). In lactating condition, the β cell mass, β cell proliferation, and insulin secretory function per islet were decreased in *Tph1* βiKO mice, but pancreas weight of *Tph1* βiKO mice was comparable to control mice (Fig. 3, I to K, and fig. S5B). However, electron microscopic analysis did not show any ultrastructural changes except that rod-shaped insulin granules were frequently observed in β cells of *Tph1* βiKO mice (fig. S5C). No phenotypic difference was seen between control and *Tph1* βiKO mice in non-lactating condition (fig. S5, D to H). These data indicate that 5-HT is necessary to induce β cell proliferation and maintain β cell function for the improvement of glycemic control during lactation.

Among the HTRs, HTR2B is known to mediate 5-HT–induced β cell proliferation and insulin secretory function, although we did not observe any lactation-related change in the expression of HTR transcripts (fig. S6A) (*20*, *28*). Therefore, we generated β cell–specific *Htr2b* KO (*Htr2b* βKO) mice in search for the downstream HTR(s) involved in β cell proliferation and function during lactation. In contrast to *Tph1* βiKO mice, glucose tolerance did not deteriorate and no ultrastructural defect was observed in *Htr2b* βKO mice during lactation (Fig. 3L and fig. S6B). However, insulin secretion, β cell mass, and β cell proliferation were decreased, whereas pancreas weight and insulin sensitivity were unaltered, in lactating *Htr2b* βKO mice compared to control mice (Fig. 3, M to P, and fig. S6, C and D). No phenotypic difference was observed in non-lactating *Htr2b* βKO mice compared to control mice (fig. S6, E to I). These data indicate that 5-HT increases β cell mass by stimulating β cell proliferation through HTR2B during lactation. In addition, the differences in glucose tolerance and ultrastructure between the *Tph1* βiKO and *Htr2b* βKO mice suggested that a more complex mechanism may be responsible for the deterioration of glucose tolerance in *Tph1* βiKO mice. This notion prompted us to further explore the possible role of 5-HT in β cell function.

5-HT protects β cells against oxidative stress

The synthesis and secretion of insulin impose a heavy demand for adenosine triphosphate (ATP) production in β cells, which are thus at a high risk of oxidative stress due to the reactive oxidative species (ROS) formation that occurs during ATP production. Tryptophan and its metabolites (5-HTP, 5-HT, and melatonin) are indole derivatives that can act as antioxidants by scavenging ROS (*29*). Therefore, we postulated that 5-HT could have a protective role in β cells by reducing oxidative stress. To test this hypothesis, we administered alloxan, a commonly used diabetogenic toxin, to mice to induce oxidative stress in β cells. At 3 days after alloxan treatment, non-lactating mice developed hyperglycemia, and their islets were destroyed with extensive β cell death, whereas the lactating mice maintained normoglycemia and preserved their β cells (Fig. 4, A and B). To further test whether 5-HT can protect β cells from oxidative stress, we administered alloxan to RIP-Cre^{Mgn} mice that produce 5-HT in their β cells (*30*, *31*). Alloxan could not induce hyperglycemia in RIP-Cre^{Mgn} mice, and their β cells were protected from alloxan-induced cell death (Fig. 4, C and D). We further assessed a direct correlation between 5-HT production and the ROS in β cells after 6 hours of alloxan administration (Fig. 4, E and F). Immunofluorescence staining for 8-oxo-2′-deoxyguanosine (8-oxo-dG), a product of DNA oxidation used as a marker for ROS, showed that ROS were present in most of the β cells of non-lactating mice (Fig. 4E). However, 8-oxo-dG was exclusively detected in 5-HT–negative β cells of lactating mice and RIP-Cre^{Mgn} mice. In *Tph1* βiKO mice, 8-oxo-dG was detected in most β cells, although these mice were lactating. In accordance with these results, terminal deoxynucleotidyl transferase–mediated deoxyuridine triphosphate nick end labeling (TUNEL) staining revealed that alloxan induced cell death only in 5-HT–negative β cells (Fig. 4F). Thus, intracellular ROS concentrations and cellular mortality were negatively correlated with intracellular 5-HT concentrations. Furthermore, direct measurement of intracellular ROS in β cells using dihydroethidium

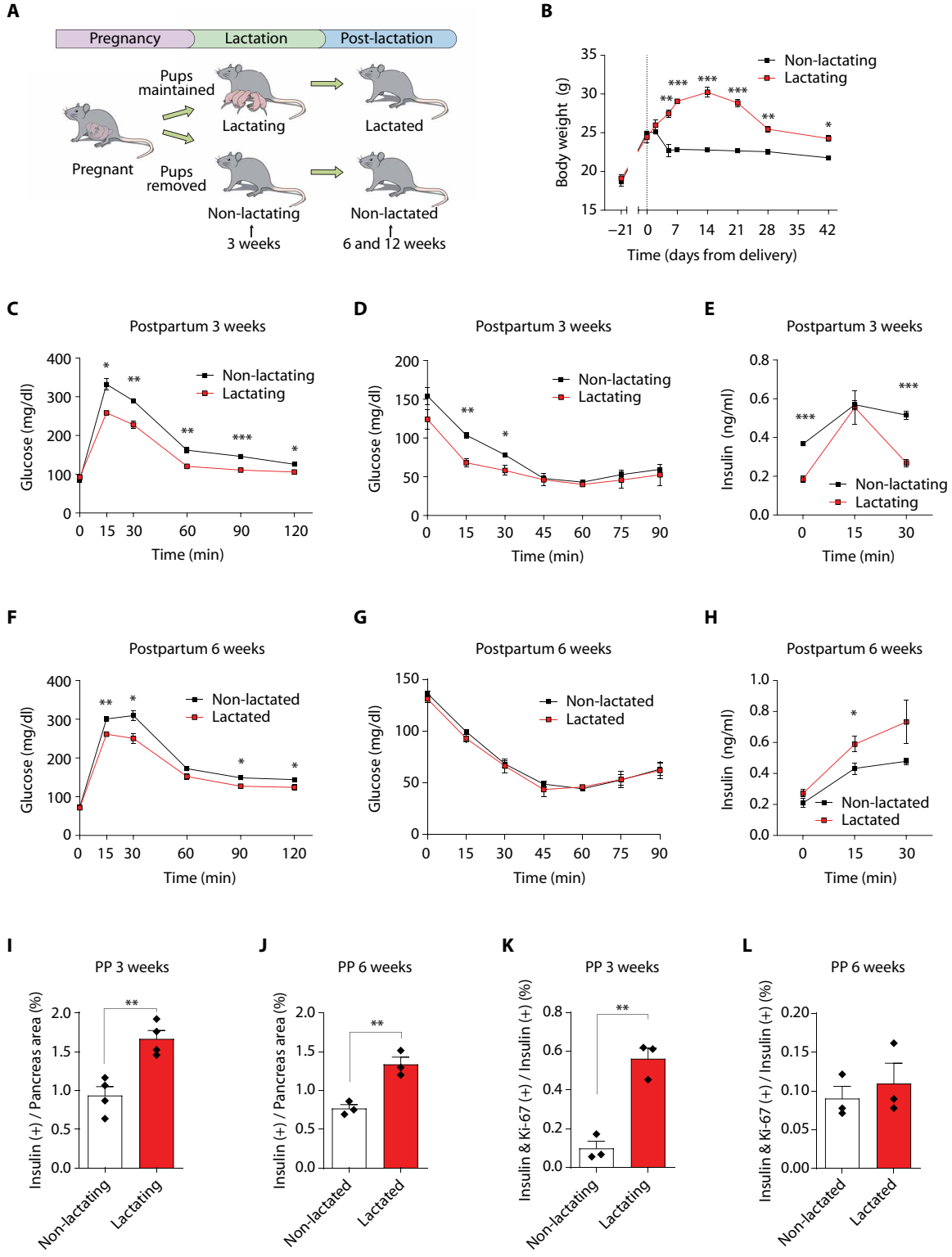

Fig. 2. Lactation improves glucose homeostasis and β cell function in mice. (**A**) Scheme of the mouse model for lactation. Female C57BL/6J mice were randomized to either lactating or non-lactating groups, and the metabolic phenotypes were evaluated at 3, 6, and 12 weeks after delivery. (**B**) Body weight by lactation status. $n = 3$ or 4 mice per time point. (**C** to **H**) Metabolic phenotypes of (C to E) lactating mice at 3 weeks postpartum and (F to H) lactated mice at 6 weeks postpartum. $n = 3$ or 4 mice per group. (C and F) Intraperitoneal glucose tolerance test (2 g/kg) after an overnight fasting. (D and G) Intraperitoneal ITT (0.75 U/kg) after a 6-hour fasting. (E and H) Plasma insulin concentrations were measured after intraperitoneal glucose injection (2 g/kg). (**I** and **J**) β cell mass was quantified as the percentage of the insulin-positive area relative to the area of the whole pancreas at (I) 3 weeks and (J) 6 weeks postpartum (PP). $n = 3$ or 4 mice per group. (**K** and **L**) β Cell proliferation rate as the percentage of insulin and Ki-67 co-positive cells relative to all insulin positive cells at (K) 3 weeks and (L) 6 weeks postpartum. $n = 3$ mice per group. Data are means ± SEM. $^*P < 0.05$, $^{**}P < 0.01$, and $^{***}P < 0.001$.

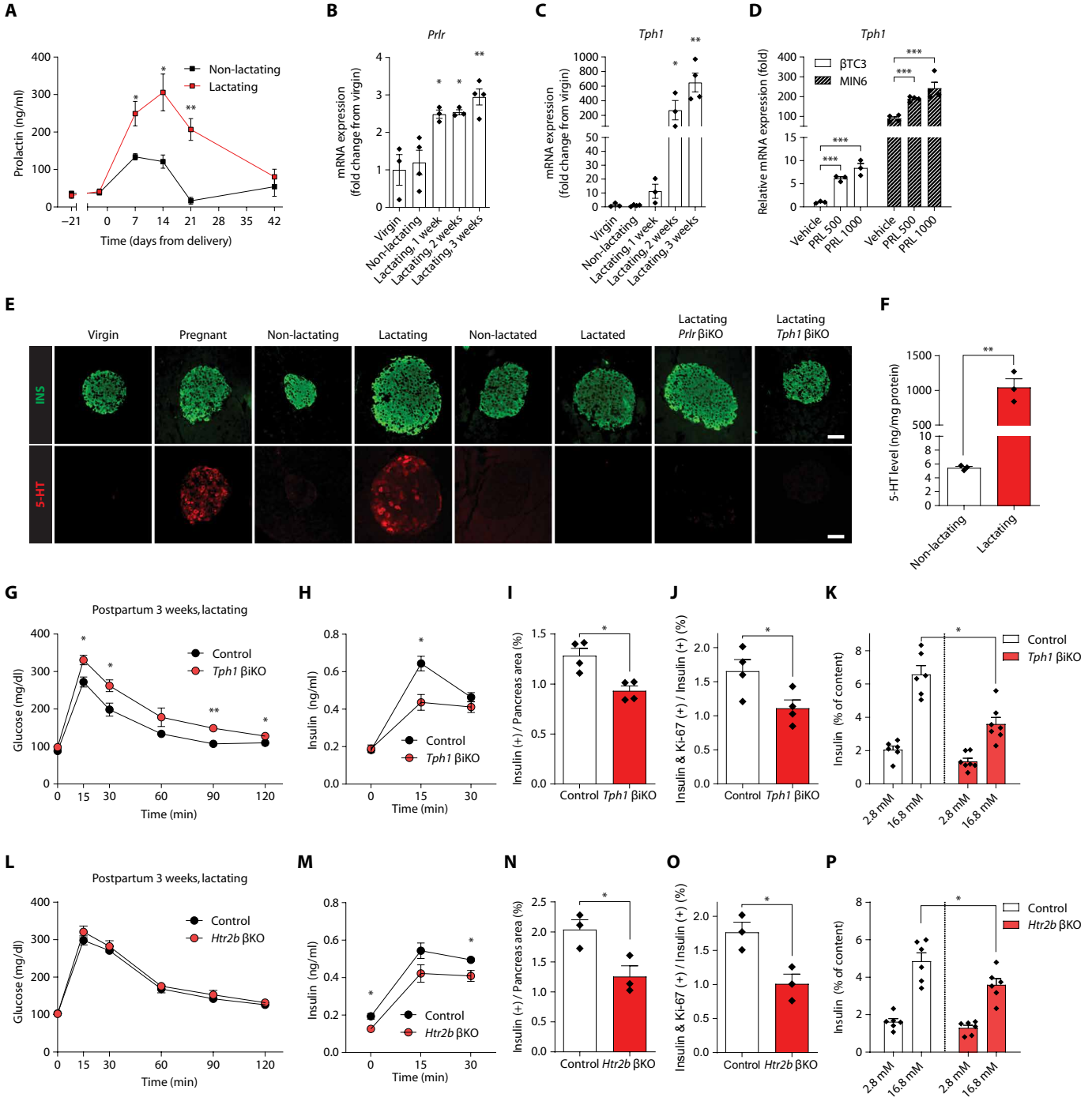

Fig. 3. 5-HT improves β cell function during lactation. (**A**) Plasma prolactin concentrations were measured using ELISA and compared by lactation status. $n = 3$ or 4 mice per time point. (**B** and **C**) mRNA expressions of (B) *Prlr* and (C) *Tph1* in lactating pancreatic islets were assessed by qRT-PCR. $n = 3$ or 4 mice per group. (**D**) mRNA expressions of *Tph1* in βTC3 and MIN6 cells treated with prolactin (ng/ml) for 24 hours were assessed by qRT-PCR. $n = 3$ or 4 replicates. (**E**) Representative immunofluorescence images of pancreatic islets obtained from C57BL/6J, *Prlr* βiKO, and *Tph1* βiKO mice during and after lactation and stained for insulin (green) and 5-HT (red). Islets from virgin mice were used as a negative control, and islets from pregnant mice were used as a positive control. Scale bar, 50 μm. (**F**) ELISA was used to measure the 5-HT content in islets isolated from non-lactating and lactating mice. 5-HT concentrations were normalized to the protein content. $n = 3$ mice per group. (**G** to **P**) The metabolic phenotypes of (G to K) *Tph1* βiKO and (L to P) *Htr2b* βKO mice during lactation (3 weeks postpartum). $n = 4$ mice per group. (G and L) Blood glucose and (H and M) plasma insulin concentrations were measured after intraperitoneal glucose injection (2 g/kg) after an overnight fasting. (I and N) β cell mass was quantified as the percentage of the insulin-positive area relative to the area of the entire pancreas. $n = 3$ or 4 mice per group. (J and O) β Cell proliferation rate, taken as the percentage of insulin and Ki-67 co-positive cells relative to all insulin-positive cells. $n = 3$ or four mice per group. (K and P) Islets isolated from lactating mice at 3 weeks postpartum were incubated for 15 min with 2.8 or 16.8 mM glucose, and secreted insulin concentrations were measured with ELISA ($n = 10$ islets/well). Insulin secretion was normalized to the total insulin content extracted from the islets. $n = 6$ replicates per group. Data are means ± SEM. $^*P < 0.05$, $^{**}P < 0.01$, and $^{***}P < 0.001$.

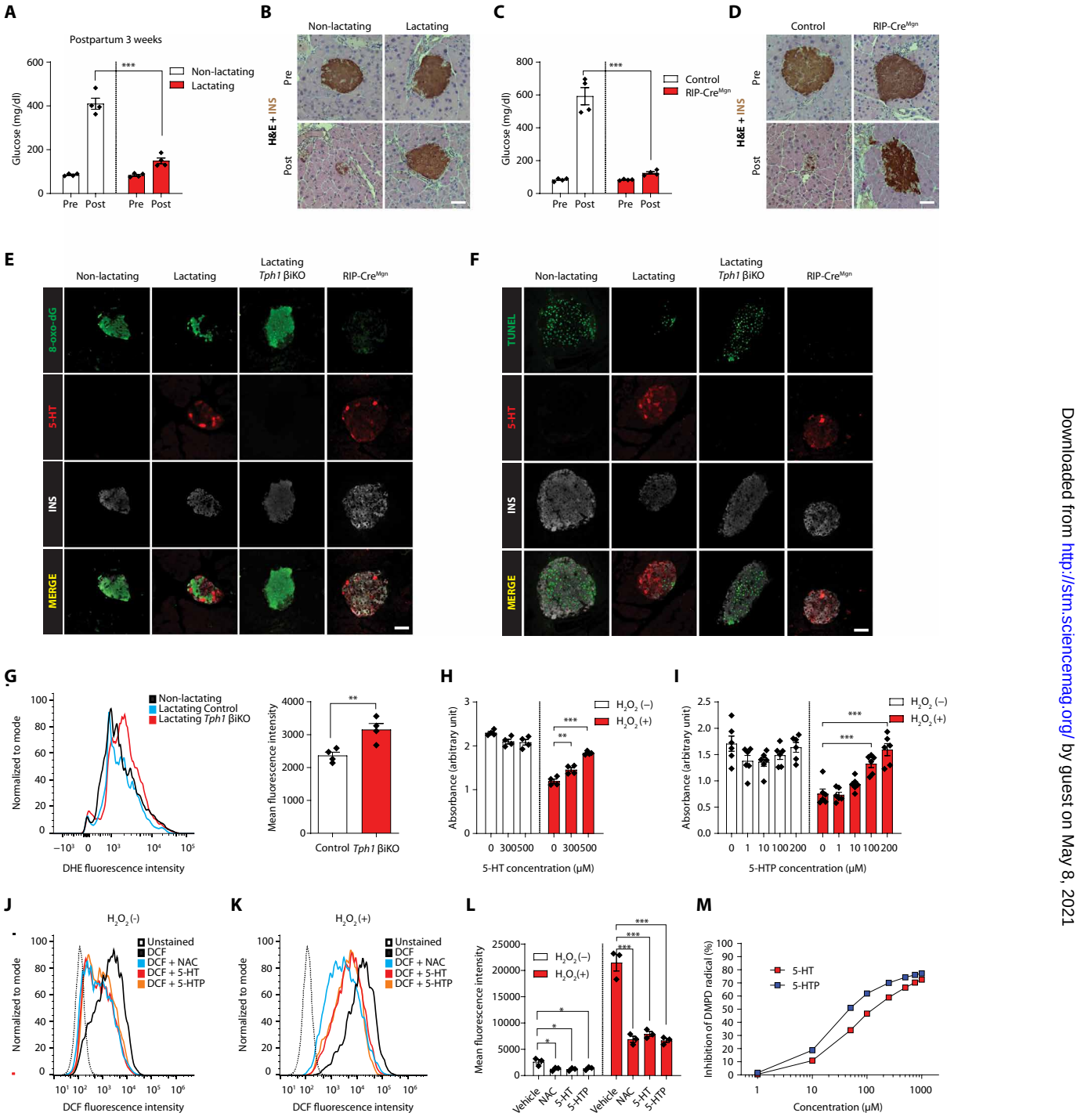

Fig. 4. 5-HT protects β cells against oxidative stress. (**A** to **F**) Alloxan was administered to induce oxidative stress in β cells of non-lactating/lactating C57BL/6J, lactating *Tph1* βiKO, and RIP-Cre^{Mgn} mice (150 mg/kg mouse). $n = 4$ mice per group. (A and C) Random glucose concentrations and (B and D) immunohistochemistry for insulin (brown) before and 3 days after alloxan injection (150 mg/kg mouse) in (A and B) non-lactating/lactating C57BL/6J mice and (C and D) control/RIP-Cre^{Mgn} mice. (E and F) Representative immunofluorescence images for (E) 8-oxo-dG (green) or (F) TUNEL (green) at 6 hours after injection of alloxan (150 mg/kg mouse) in non-lactating/lactating C57BL/6J, lactating *Tph1* βiKO, and RIP-Cre^{Mgn} mice (5-HT in red; insulin in gray). (**G**) Flow cytometry was used to measure intracellular ROS as the DHE fluorescence intensity in β cells of lactating *Tph1* βiKO mice. Mean fluorescence intensity is depicted in the right panel for quantitative analysis. Islets from three or more mice were pooled for each data point. The experiment was repeated four times. (**H** and **I**) Cell survival was measured by MTT assay in *Tph1*-null MIN6 cells treated with (H) 5-HT and (I) 5-HTP in the presence or absence of H_2O_2 (200 μM). $n = 4$ to 6 replicates per group. (**J** to **L**) Flow cytometry was used to measure the intracellular ROS as the DCF-DA fluorescence intensity in *Tph1*-null MIN6 cells treated with 5-HT (500 μM) and 5-HTP (200 μM) (J) without and (K) with H_2O_2. *N*-acetylcysteine (NAC) (5 mM) was used as a control. $n = 3$ replicates per group. (L) Mean fluorescent intensity for (J and K) is depicted for quantitative analysis. $n = 3$ replicates per group. (**M**) In vitro free radical scavenging activity was measured by the ratio of DMPD radical inhibited by 5-HT and 5-HTP. $n = 4$ replicates per group. Data are means ± SEM. $^*P < 0.05$, $^{**}P < 0.01$, and $^{***}P < 0.001$.

(DHE) revealed that the intracellular ROS concentrations were higher in lactating *Tph1* βiKO mice than in wild-type lactating mice (Fig. 4G). These data suggest that 5-HT has antioxidant activity in lactating β cells.

To test the antioxidant activity of 5-HT derivatives (5-HT and 5-HTP), we established *Tph1*-null MIN6 cells in which endogenous 5-HT synthesis was abolished (fig. S7A). The entry of 5-HT/5-HTP into *Tph1*-null MIN6 cells upon treating them with 5-HT/5-HTP was confirmed by detecting intracellular 5-HT by immunofluorescence staining and enzyme-linked immunosorbent assay (ELISA) (fig. S7, B and C). The mRNA transcripts of monoamine transporters (*Slc29a4* and *Slc18a1*) were detected in MIN6 cells, suggesting a route through which 5-HT/5-HTP could enter the cells (fig. S7D). The intracellular 5-HT concentration of lactating islets was similar to that of *Tph1*-null MIN6 cells treated with 10 to 50 μM 5-HT. Considering the heterogeneous and stochastic pattern of 5-HT expression during lactation and the potential for underestimating 5-HT due to its degradation during islet isolation, cells treated with ≥50 μM 5-HT would represent intracellular 5-HT concentration similar to that of individual lactating β cells that actively produce 5-HT (Fig. 3, E and F, and fig. S7C). H_2O_2 induced cell death in *Tph1*-null MIN6 cells, which were rescued with increasing concentrations of 5-HT and 5-HTP (Fig. 4, H and I). Both 5-HT and 5-HTP reduced the intracellular ROS regardless of H_2O_2 treatment (Fig. 4, J to L, and fig. S7E). Moreover, the phosphorylation of c-Jun N-terminal kinase (JNK) and cleaved caspase 3 were reduced by 5-HTP treatment in *Tph1*-null MIN6 cells (fig. S7F).

Next, we investigated whether 5-HT derivatives can directly scavenge ROS. An in vitro free radical scavenging activity assay confirmed that 5-HT and 5-HTP had direct antioxidant properties (Fig. 4M). However, the expression of antioxidant genes was not notably changed upon 5-HT treatment in *Tph1*-null MIN6 cells except for *Sod3*, *Gpx2*, and *Gpx3* (fig. S7G). The expression of antioxidant genes was not increased in lactating islets, except a modest increase in *Gpx1*, or decreased in *Tph1* βiKO islets, suggesting that the antioxidant effects of 5-HT were not mediated through the increased expression of antioxidant genes (fig. S7, H and I). These data collectively suggest that 5-HT derivatives protect β cells against oxidative stress by directly scavenging ROS.

DISCUSSION

Women experience physiologic but severe insulin resistance during pregnancy, and this can threaten their metabolic health after delivery. Therefore, the management of maternal metabolic risk factors in the peripartum period is important. Previous epidemiological studies have reported that lactation has beneficial effects on maternal metabolic health. In the Nurses' Health Study, each additional year of lactation was found to reduce the risk of diabetes by 15% (*8*). Ziegler *et al.* (*32*) also reported that German women with gestational diabetes who lactated >3 months reduced their risk of postpartum diabetes by 46%. Improved insulin sensitivity due to increased energy consumption by lactation (~500 kcal/day) has been suggested as one mechanism underlying these beneficial effects (*12*). However, the lack of translational studies has limited further mechanistic investigation into the metabolic aspect of maternal physiology.

In the present study, we evaluated the metabolic phenotypes of humans and mice during lactation and after the cessation of lactation and identified the long-term beneficial effects of lactation on β cell mass and function (fig. S8). During lactation, circulating prolactin binds to PRLR and activates the PRLR-STAT5-TPH1 cascade to stimulate 5-HT production in β cells. In turn, 5-HT stimulates β cell proliferation through HTR2B in an autocrine/paracrine manner. In addition, intracellular 5-HT scavenges ROS from β cells and mitigates intracellular oxidative stress. These beneficial effects of lactation on β cell mass and function last for years after the cessation of lactation, thereby improving women's metabolic health.

The production of 5-HT in human β cells has been reported by multiple groups (*20*, *33*–*35*). A recent study by Martin-Montalvo *et al.* (*36*) reported that human islets respond to prolactin to produce *TPH1*. In addition, higher gestational serum prolactin concentration is correlated with improved β cell function and a lower risk of postpartum diabetes in women (*37*). These studies at least partially support the idea that prolactin-induced 5-HT production in β cells contributes to the beneficial metabolic phenotypes of women undergoing lactation.

Pancreatic β cells are among the cells consuming the most ATP during the synthesis and secretion of insulin. Mitochondrial ATP production is accompanied by the generation of ROS, which impose oxidative stress on cells. Despite their high ROS production, however, β cells have lower amounts of antioxidants compared to other metabolic organs (*38*, *39*). β Cells are therefore vulnerable to oxidative stress, which eventually leads to cell death and loss of the β cell mass (*40*, *41*). Tryptophan and its metabolites (5-HTP, 5-HT, and melatonin) are indole derivatives that contain multiple double bonds in a bicyclic structure and can directly scavenge ROS as antioxidants (*29*). In addition, the tryptophan metabolism pathway includes multiple oxidation and dehydrogenation reactions, enabling its intermediates to act as reducing agents (*42*). In the present study, we demonstrated that 5-HT and 5-HTP directly scavenge ROS and enhance cell survival. 5-HT production in β cells is physiologically relevant for the reduction of cellular stress because β cells experience a heavy workload during lactation and pregnancy (*20*). Because oral 5-HTP supplementation is sufficient to increase systemic 5-HT availability and has an anti-diabetic effect, its potential implication for enhancing β cell function to prevent the progression to diabetes warrants further evaluation (*43*).

There are limitations of this study. Possible contributions of other HTRs, especially HTR3, which improves insulin secretion, should be further investigated (*21*). Recent studies indicating that HTR2B can either enhance or perturb glucose-stimulated insulin secretion and mitochondrial respiration suggest another possible contribution of 5-HT to mitochondrial function (*28*, *44*–*46*). It is not certain whether ROS is a complication of pregnancy or lactation. However, the amount of ROS in lactating islets is comparable to that in non-lactating islets, which was higher in lactating *Tph1* βiKO islets. These data indirectly suggest that ROS production increases during pregnancy or lactation, but 5-HT simultaneously scavenges the ROS in β cells. The measurement of dynamic changes in ROS during pregnancy or lactation needs to be further evaluated.

In summary, lactation benefits women's metabolic health by improving β cell mass and function and glycemic control. 5-HT plays a critical role in achieving the necessary β cell mass during lactation by stimulating β cell proliferation and exerting an antioxidant activity to protect β cells against oxidative stress. Future studies on the modulation of the serotonergic pathway in accordance with the management of maternal metabolic risk factors would provide additional insights into maternal physiology.

MATERIALS AND METHODS

Study design

The objective of this study was to investigate the mechanism underlying the long-term beneficial effects of lactation on future diabetes risk. To obtain human data, we conducted a multicenter prospective cohort study among subjects with a first-time diagnosis of gestational diabetes mellitus (GDM) or GIGT. Subjects with overt type 2 diabetes or persistent diabetes at the initial postpartum visit were excluded. A total of 174 subjects were included in this study without a specific endpoint. Participants decided whether to lactate according to their will, and researchers were not blinded to their lactation status. For animal studies, mice were randomly assigned to either lactating or non-lactating groups (n = 3 to 6 per group). Researchers were blinded to the animals' genotype and the lactation status.

Human studies

All pregnant women were screened for GDM with a 50-g oral glucose challenge test between 24 and 28 weeks of gestation, and a positive screen was defined as a 1-hour glucose value ≥130 mg/dl. Women with a positive screen were given a 3-hour 100-g OGTT. The diagnoses of GDM and GIGT were made using the recommendations of the Third International Workshop-Conference on Gestational Diabetes Mellitus (*47*). Two or more of the following criteria for GDM and one of the following criteria for GIGT were required for the diagnosis: fasting plasma glucose ≥105 mg/dl, 1-hour glucose ≥190 mg/dl, 2-hour glucose ≥165 mg/dl, or 3-hour glucose ≥145 mg/dl.

Women with GDM or GIGT who attended the initial postpartum evaluation were enrolled in this study (n = 282). The initial postpartum follow-up visit was performed at 2 months postpartum, and annual follow-up visits were made thereafter. Subjects who had persistent diabetes at the initial visit were excluded. Among the eligible subjects, a total of 174 (lactated, n = 85; non-lactated, n = 99) subjects completed follow-up examinations more than once and had the OGTT performed. The mean duration of the follow-up was 3.6 ± 0.1 years after delivery.

Subjects were recruited from August 1995 to May 1997 from four centers in Korea. All subjects participated voluntarily, and informed consent was obtained from each subject. This study was approved by the Institutional Review Board of Seoul National University Bundang Hospital (IRB Number: B-1903-526-107) and was conducted according to the requirements of the Declaration of Helsinki (*48*).

Postpartum follow-up examinations

Face-to-face interviews were conducted at the first postpartum examination using a standardized questionnaire that included past medical and reproductive history. Obstetric history, including parity and pregestational weight, was retrieved from the patient's medical records. For the postpartum follow-up assessment, a standard 75-g OGTT was performed at each follow-up visit. Anthropometric measures, including body weight and height, were measured at each visit.

Metabolic assessment

A metabolic assessment, including a 75-g OGTT, was performed after overnight fasting. The plasma glucose concentrations were enzymatically measured by an automated analyzer (Yellow Springs Instrument Co.) using the glucose oxidase method. The plasma insulin concentrations were measured by a radioimmunoassay (Linco Research Inc.). The insulin sensitivity was assessed by the Matsuda index as follows: $10{,}000/\sqrt{[(\text{fasting glucose}) \times (\text{fasting insulin}) \times (\text{mean glucose}) \times (\text{mean insulin})]}$ (*49*). The insulinogenic index was used to estimate insulin secretion as follows: (insulin [30 min] − insulin [0 min])/(glucose [30 min] − glucose [0 min]) (*50*). The disposition index was used to evaluate the composite of insulin secretion considering the degree of insulin sensitivity as follows: (Matsuda index) × (Insulinogenic index) (*51*).

Animal experiments

All mice used in this study were from the C57BL/6J background. The mice were housed in a specific pathogen–free facility at Korea Advanced Institute of Science and Technology with a 12-hour light and dark cycle in isothermal and isohumid conditions. A standard chow diet (D10001, Research Diets Inc.) and water were given ad libitum. All mouse studies were approved by the Institutional Animal Care and Use Committee of the Korea Advanced Institute of Science and Technology. All experiments were performed in accordance with the relevant guidelines and regulations.

For the lactation mouse model experiments, 9-week-old female C57BL/6J mice were mated for 7 days, and pregnant mice were allocated to either the "Lactating" or "Non-lactating" groups. For Lactating mice, the pups were left in the cage after delivery; for Non-lactating mice, the pups were removed from the cage on the day of delivery. The metabolic phenotypes of these mice were assessed after 3 weeks of lactation, which was calculated based on the day of parturition. The pups were weaned 3 weeks after delivery, and the dam mice were classified as either "Lactated" or "Non-lactated." A metabolic evaluation was performed at 6 weeks postpartum. The scheme is depicted in Fig. 2A. For the multiparous mouse study, 9-week-old female mice had three deliveries with/without lactation. A metabolic evaluation was performed after 8 to 12 weeks from last delivery.

To generate β cell–specific inducible KO (βiKO) mice, *Pdx1-CreER* (MGI 2684321) mice were mated with mice harboring a *Tph1* floxed allele (MGI 6271993) or a *Prlr* floxed allele (*24*, *52*, *53*). Tamoxifen (dissolved in corn oil) was intraperitoneally injected once on the day of delivery (75 mg/kg per mouse) to both control and experimental mice to induce gene KO. *Ins2-Cre* (MGI 2387567) mice were mated with *Htr2b* floxed (MGI 3837400) to create β cell–specific KO (βKO) mice (*54*–*56*). Both Cre lines lack a human growth hormone cassette and are commonly used in β cell studies (*57*). ROSA26-EYFP mice (MGI 2449038) (*58*) were crossed with β cell–specific Cre mice, which enabled us to distinguish the β cells for flow cytometric analysis and to test the specificity and efficiency of the Cre lines. The *Pdx1-CreER* line was previously validated to have little tamoxifen-independent recombination (*59*). The genotyping primers are presented in table S3. For the alloxan experiments, the mice were fasted overnight the day before the administration. Alloxan was dissolved in sodium citrate buffer (pH 4.5) (25 mg/ml), and 150 mg/kg of alloxan was injected intraperitoneally into the mice. The mice were euthanized 6 hours or 3 days after the administration of alloxan. Plasma prolactin concentrations were measured by ELISA following the manufacturer's protocol (Abcam).

Glucose dynamics

For the intraperitoneal glucose tolerance test and the in vivo glucose-stimulated insulin secretion test, the mice were fasted overnight for 16 hours, and D-glucose (2 g/kg mouse) was injected intraperitoneally. The blood glucose concentrations were measured from the tail vein using a glucometer (GlucoDr Plus, Allmedicus). For the insulin measurement, blood was collected 0, 15, and 30 min after glucose

injection in a heparinized tube, which was immediately centrifuged at 1500*g* for 10 min at 4°C. The plasma insulin concentration was measured using an ultrasensitive insulin ELISA kit (ALPCO). The insulinogenic index was calculated as the increase in the plasma insulin concentrations over the change in the blood glucose concentrations upon glucose administration during the in vivo glucose-stimulated insulin secretion test: (insulin [15 min] − insulin [0 min])/(glucose [15 min] − glucose [0 min]). For the insulin tolerance test (ITT), the mice were fasted for 6 hours before an intraperitoneal Humulin R (Eli Lilly) injection (0.75 U/kg body weight).

Islet studies

Mouse islets were isolated in the conventional manner using collagenase as described previously (*60*). For quantitative reverse transcription polymerase chain reaction (qRT-PCR) analysis, islets were handpicked after the isolation and were simultaneously transferred to TRIzol for RNA extraction.

For the ex vivo glucose-stimulated insulin secretion test, the islets were incubated at 37°C in a humidified chamber of 5% CO_2 and 95% air in RPMI 1640 medium (Thermo Fisher Scientific) with penicillin-streptomycin (100 U/ml) (Thermo Fisher Scientific) and 10% fetal bovine serum (FBS) (Thermo Fisher Scientific). After 4 hours of incubation, the islets were moved to Krebs-Ringer-Hepes (KRH) buffer [pH 7.4, 115 mM NaCl, 25 mM Hepes, 24 mM $NaHCO_3$, 5 mM KCl, 1 mM $MgCl_2$, 2.5 mM $CaCl_2$, and bovine serum albumin (BSA) (1 mg/ml)] containing 2.8 mM glucose for 30 min. The islets were handpicked (n = 10 islets per individual sample) and placed into a 12-well noncoated dish. To measure the basal insulin secretion, the samples were incubated with 2.8 mM glucose containing KRH buffer for 15 min, and 50 μl of supernatant was obtained for the insulin measurements. For high-glucose stimulation, the samples were incubated with 16.8 mM glucose containing KRH buffer for 15 min, and the supernatants were obtained. Next, the islets were sonicated and incubated in acid-ethanol (1.5% HCl in 100 ml of 70% ethanol) for 18 hours at 4°C for intracellular insulin extraction. The same volume of 1 M tris-Cl buffer (pH 8.0) was added for neutralization. All supernatants were immediately snap-frozen with liquid nitrogen and were kept frozen at −80°C until the ELISA experiments. Insulin secretion was normalized to the content of insulin extracted from the islets.

Immunostaining and β cell mass and proliferation measurements

Mouse pancreatic tissues were fixed immediately after being harvested in a 10% neutral-buffered formalin solution (Sigma) for 4 hours at room temperature and were washed with type 3 water for 30 min. After washing, the pancreatic tissues were dehydrated with a tissue processor (Leica) and were embedded in paraffin. The formalin-fixed, paraffin-embedded tissues were sectioned into 4-μm-thick slices and mounted onto glass slides. These slides were manually deparaffinized in xylene and rehydrated in ethanol for further staining. Antigen retrieval was performed with sodium citrate buffer (10 mM sodium citrate, pH 6.0) with a pressure cooker for 15 min.

For immunofluorescent staining, the samples were blocked with 2% donkey serum diluted in phosphate-buffered saline (PBS) for 1 hour at room temperature. The primary antibody–treated slides were incubated at 4°C overnight with the following antibodies: anti–5-HT antibody (rabbit, ImmunoStar, dilution factor 1:1000), anti–8-oxo-dG antibody (mouse, Abcam, 1:200), anti-insulin antibody (guinea pig, Dako, 1:500), and anti–Ki-67 antibody (rabbit, Abcam, 1:1000). After incubation and washing, the secondary antibodies were added, and the slides were incubated for 2 hours at room temperature as follows: Alexa Fluor 488–conjugated donkey anti-mouse immunoglobulin G (IgG) (Jackson ImmunoResearch, 1:500), Alexa Fluor 594–conjugated donkey anti-rabbit IgG (Jackson ImmunoResearch, 1:500), and Alexa Fluor 647–conjugated donkey anti–guinea pig IgG (Jackson ImmunoResearch, 1:500). TUNEL staining was performed after immunofluorescent staining according to the manufacturer's protocol (In Situ Cell Death Detection Kit, Fluorescein, Roche). The samples were treated with 4′,6-diamidino-2-phenylindole (DAPI) (Invitrogen, 1:2000) for 5 min and mounted with fluorescence mounting medium (Dako).

For immunohistochemistry staining, the sections were incubated with BLOXALL (Vector Laboratories) at room temperature for 10 min and blocked with 2% serum and treated with the primary antibodies as above. After washing, biotinylated secondary antibody was incubated with the samples for 30 min at room temperature, and immunohistochemistry was performed using the VECTASTAIN ABC kit and DAB following the manufacturer's protocol (Vector Laboratories). The slides were counterstained with hematoxylin and eosin. All pictures were obtained using a confocal microscope LSM780 (Carl Zeiss) or a fluorescence microscope with a DS-Ri2 camera (Nikon).

For the β cell mass measurements, formalin-fixed, paraffin-embedded pancreas slides were obtained with an 80-μm interval (minimum eight slides per mouse). These slides were immunostained with insulin, and the whole slides were scanned with JuLI stage (NanoEnTek). The β cell mass was measured as the insulin immunoreactive area divided by the whole pancreas area. Multiplying the pancreas weight by the β cell area did not alter our conclusions. Therefore, we used the β cell area as a measure for the β cell mass. For the β cell proliferation measurements, the above slides were immunostained with insulin and Ki-67. The β cell proliferation rate was calculated as the percentage of insulin and Ki-67 co-positive cells over all β (insulin-positive) cells.

Quantitative reverse transcription polymerase chain reaction

RNA was extracted using TRIzol (Invitrogen) following the manufacturer's protocol. One microgram of total RNA was used to generate complementary DNA (cDNA) with the High-Capacity cDNA Reverse Transcription Kit (Applied Biosystems). qRT-PCR was performed with Fast SYBR Green Master Mix (Applied Biosystems) using the ViiA 7 Real-time PCR System (Applied Biosystems). The gene expression was calculated by relative gene expression analysis using the ΔC_t (threshold cycle) method. *Actb* was used as an internal control. The primers used in these experiments are presented in table S4.

Cell culture and generation of *Tph1*-null MIN6 cells using CRISPR/Cas9

MIN6 cells were incubated in Dulbecco's modified Eagle's medium (DMEM) containing 25 mM glucose (HyClone) supplemented with 15% FBS, penicillin (100 U/ml), streptomycin (0.1 mg/ml), and 71.5 μM 2-mercaptoethanol. βTC3 cells were incubated in DMEM containing 25 mM glucose supplemented with 10% FBS, penicillin (100 U/ml), and streptomycin (0.1 mg/ml). The cells were incubated at 37°C in a humidified incubator containing 5% CO_2. The cells were incubated in serum-free medium for 16 hours before and during prolactin treatment. The cells were treated with recombinant mouse prolactin

(National Hormone and Peptide Program) for 24 hours before RNA was extracted.

Tph1-null MIN6 cells were generated by the method described by Sanjana *et al.* (*61*) and Shalem *et al.* (*62*). The lentiCRISPR v2 was a gift from F. Zhang (Addgene plasmid #52961). The *Tph1*-specific guide RNA was designed using the CRISPR design tool (http://crispr.mit.edu/), which was shown to have minimal off-target effects (*63*). The sequences of oligo DNA are described in table S4. No potential off-target site was found using the in silico tool Cas-OFFinder (*64*). A 2-kb filler of the lentiCRISPR v2 vector was replaced by annealed oligos. Then, lentiCRISPR v2–Tph1 was transfected into MIN6 cells, and the stably transfected cells were selected by puromycin (10 μg/ml) treatment for at least 2 weeks. For 5-HT measurement, isolated islets and cells were lysed in radioimmunoprecipitation assay (RIPA) buffer (Thermo Fisher Scientific), sonicated, and centrifuged at 12,000*g* for 5 min at 4°C. 5-HT was measured in supernatants using a commercial ELISA kit (LDN) as described by the manufacturer. The protein content was concomitantly measured using the BCA assay technique (Thermo Fisher Scientific), and the 5-HT content was normalized to the total protein content.

Immunoblot analysis

The immunoblot analysis was performed as previously described (*53*). The cells were lysed in RIPA buffer with a protease inhibitor cocktail (Sigma-Aldrich). The protein concentration was measured using the Pierce BCA Protein Assay Kit (Thermo Fisher Scientific). The proteins in whole-cell lysates were separated by SDS–polyacrylamide gel electrophoresis (SDS-PAGE) on a 10% polyacrylamide gel and transferred to a polyvinylidene difluoride membrane (Merck Millipore). The membrane was blocked in 1% (w/v) BSA in TBS-T (150 mM sodium chloride, 20 mM tris, 0.1% Tween 20, pH 7.6) and was incubated with a rabbit anti-TPH1 antibody (1:1000; Cell Signaling, #12339), a rabbit anti-cleaved caspase 3 antibody (1:1000, Cell Signaling, #9664), a rabbit anti–phospho-SAPK (stress-activated protein kinase)/JNK antibody (1:1000; Cell Signaling, #9251), or a mouse anti–β-actin antibody (1:5000, Cell Signaling, #3700) overnight at 4°C. After washing three times in TBS-T (10 min each) at room temperature, the membrane was incubated with a horseradish peroxidase (HRP)–conjugated anti-rabbit IgG secondary antibody (1:5000; Cell Signaling, #7074) or an anti-mouse IgG antibody (1:5000, Cell Signaling, #7076) for 1 hour. After washing three times in TBS-T (10 min each) at room temperature, the immunoreactive proteins were detected using the Immobilon Western Chemiluminescent HRP Substrate (Merck Millipore). The images were analyzed using the ChemiDoc MP System (Bio-Rad).

Cell viability assay

The cell viability was analyzed by an MTT [3-(4,5-dimethylthiazol-2-yl)-2,5-diphenyltetrazolium bromide] assay. *Tph1*-null MIN6 cells were plated in 24-well culture plates. The cells were treated with 5-HT or 5-HTP for 24 hours under serum-free conditions, and then hydrogen peroxide (final concentration of 200 μM) was added. After 6 hours of incubation, the MTT solution (5 mg/ml in PBS) was added at a 1:10 ratio and was incubated for 1 hour at 37°C. After discarding the medium, the formazan crystals were dissolved in dimethyl sulfoxide. Absorbance at 560 nm was measured using Multiskan GO (Thermo Fisher Scientific).

Flow cytometry and intracellular ROS measurement

To measure the intracellular ROS in isolated islets, the islets were incubated in serum-free RPMI with DHE (final concentration of 10 μM) for 30 min in a noncoated dish. The islets were dissociated into single cells with 0.25% trypsin-EDTA (HyClone) in a rotator in a 37°C incubator for 5 min. The dissociated islet cells were dispersed in phenol-free RPMI containing 0.1% BSA and filtered with a round-bottom tube with a cell strainer (Falcon), and the intensity of DHE fluorescence was measured with flow cytometry (BD LSRFortessa).

The ROS concentrations in hydrogen peroxide–treated *Tph1*-null MIN6 cells were measured by 2,7-dichlorofluorescein diacetate (DCF-DA) assay. *Tph1*-null MIN6 cells were treated with 5-HT, 5-HTP, or *N*-acetylcysteine (NAC) for 24 hours in serum-free conditions and then treated with DCF-DA for 30 min (final concentration, 50 μM). The media were discarded, and the cells were washed once in PBS. The cells were incubated in DMEM with or without hydrogen peroxide (200 μM) containing 5-HT (500 μM), 5-HTP (200 μM), or NAC (5 mM). After 30 min of incubation, the cells were detached with trypsin-EDTA. The cells were filtered with a round-bottom tube with a cell strainer (Falcon), and the intensity of DCF-DA fluorescence was measured by flow cytometry (BD LSRFortessa).

In vitro free radical scavenging activity assay

The DMPD (*N*,*N*-dimethyl-*p*-phenylenediamine dihydrochloride) assay was modified from the method described by Fogliano *et al.* (*65*). One milliliter of 100 mM DMPD solution was added to 100 ml of 0.1 M acetate buffer (pH 5.25). Then, 0.2 ml of 0.05 M ferric chloride solution was added to generate the DMPD radical cation. Twenty microliters of 5-HT and 5-HTP (final concentration range: 1 to 1000 μM) was placed in a 96-well microplate, and then 180 μl of colored DMPD radical solution was added. After incubation for 10 min at 25°C, the absorbance at 505 nm was measured. DMPD radical inhibition was calculated as follows:

$$\text{Inhibition of } A_{505\,\text{nm}}\,(\%) = (1 - A_f/A_0) \times 100$$

A_0 is the absorbance of the uninhibited radical cation, and A_f is the absorbance measured 10 min after the addition of 5-HT or 5-HTP.

Transmission electron microscopy

Isolated mouse pancreatic islets were pelleted by centrifugation and fixed in 2.5% glutaraldehyde solution in a phosphate buffer (0.1 M, pH 7.4) for 2 hours at 4°C. The islets were repelleted, washed with phosphate buffer, and then postfixed in 1% osmium tetroxide (Electron Microscopy Sciences) for 1 to 2 hours at 4°C. The samples were washed with distilled water before en bloc staining in 2% aqueous uranyl acetate. After an overnight incubation, the samples were dehydrated in a graded ethanol series, followed by propylene oxide, and then progressively infiltrated by a 2:1, 1:1, and 1:2 mixture of propylene oxide and Epon 812 resin (EMS). The samples were finally embedded in 100% Epon 812 resin and polymerized at 70°C for 24 hours. Ultrathin plastic sections (80 nm thick) were cut at room temperature using a Leica EM UC6 ultramicrotome (Leica Microsystems GmbH), collected on 200-mesh carbon-coated grids, and examined under Zeiss LEO912AB TEM (Carl Zeiss) and FEI Tecnai G2 Spirit TWIN TEM (FEI Company) at an accelerating voltage of 120 kV.

Statistical analysis

All data are presented as the mean ± SEM for continuous variables or as a number (percentage) for nominal variables. The statistical significance was calculated by Student's *t* test (two-tailed) or analysis

of variance (ANOVA) (Tukey's HSD for post hoc) for continuous variables and the χ^2 test for categorical variables. Statistical analyses were conducted using SPSS version 22 (IBM Co). Statistical significance is indicated as $^*P < 0.05$, $^{**}P < 0.01$, and $^{***}P < 0.001$. Raw data are provided in data file S1.

SUPPLEMENTARY MATERIALS

stm.sciencemag.org/cgi/content/full/12/541/eaay0455/DC1
Fig. S1. Metabolic phenotypes of lactating and lactated mice.
Fig. S2. β Cell characteristics during and after lactation.
Fig. S3. Ex vivo glucose-stimulated insulin secretion of isolated islets from lactating/lactated mice.
Fig. S4. The specificity and efficiency of *Cre* lines.
Fig. S5. Metabolic phenotypes of *Tph1* βiKO mice.
Fig. S6. Metabolic phenotypes of *Htr2b* βKO mice.
Fig. S7. Establishment of *Tph1*-null MIN6 cell line and antioxidant properties of 5-HT.
Fig. S8. Schematic summary of this study.
Table S1. Baseline characteristics and glycemic profiles during gestation.
Table S2. Glycemic profiles of the 75-g OGTT during and after lactation.
Table S3. Primer sequences for genotyping.
Table S4. Primer sequences for qRT-PCR and CRISPR KO.
Data file S1. Raw data.

View/request a protocol for this paper from *Bio-protocol*.

REFERENCES AND NOTES

1. D. A. Pyke, Parity and the incidence of diabetes. *Lancet* **270**, 818–820 (1956).
2. P. Li, Z. Shan, L. Zhou, M. Xie, W. Bao, Y. Zhang, Y. Rong, W. Yang, L. Liu, Mechanisms in endocrinology: Parity and risk of type 2 diabetes: A systematic review and dose-response meta-analysis. *Eur. J. Endocrinol.* **175**, R231–R245 (2016).
3. C. Kim, K. M. Newton, R. H. Knopp, Gestational diabetes and the incidence of type 2 diabetes: A systematic review. *Diabetes Care* **25**, 1862–1868 (2002).
4. J. H. Moon, S. H. Kwak, H. S. Jung, S. H. Choi, S. Lim, Y. M. Cho, K. S. Park, H. C. Jang, N. H. Cho, Weight gain and progression to type 2 diabetes in women with a history of gestational diabetes mellitus. *J. Clin. Endocrinol. Metab.* **100**, 3548–3555 (2015).
5. G. A. Colditz, W. C. Willett, A. Rotnitzky, J. E. Manson, Weight gain as a risk factor for clinical diabetes mellitus in women. *Ann. Intern. Med.* **122**, 481–486 (1995).
6. J. H. Moon, S. H. Kwak, H. C. Jang, Prevention of type 2 diabetes mellitus in women with previous gestational diabetes mellitus. *Korean J. Intern. Med.* **32**, 26–41 (2017).
7. B. Liu, L. Jorm, E. Banks, Parity, breastfeeding, and the subsequent risk of maternal type 2 diabetes. *Diabetes Care* **33**, 1239–1241 (2010).
8. A. M. Stuebe, J. W. Rich-Edwards, W. C. Willett, J. E. Manson, K. B. Michels, Duration of lactation and incidence of type 2 diabetes. *JAMA* **294**, 2601–2610 (2005).
9. E. P. Gunderson, C. E. Lewis, Y. Lin, M. Sorel, M. Gross, S. Sidney, D. R. Jacobs Jr., J. M. Shikany, C. P. Quesenberry Jr., Lactation duration and progression to diabetes in women across the childbearing years: The 30-year CARDIA study. *JAMA Intern. Med.* **178**, 328–337 (2018).
10. N. F. Butte, W. W. Wong, J. M. Hopkinson, Energy requirements of lactating women derived from doubly labeled water and milk energy output. *J. Nutr.* **131**, 53–58 (2001).
11. N. F. Butte, J. M. Hopkinson, Body composition changes during lactation are highly variable among women. *J. Nutr.* **128**, 381S–385S (1998).
12. A. I. Eidelman, R. J. Schanler, Breastfeeding and the use of human milk. *Pediatrics* **129**, e827–e841 (2012).
13. M. D. Gershon, L. L. Ross, Location of sites of 5-hydroxytryptamine storage and metabolism by radioautography. *J. Physiol.* **186**, 477–492 (1966).
14. F. Côté, E. Thévenot, C. Fligny, Y. Fromes, M. Darmon, M.-A. Ripoche, E. Bayard, N. Hanoun, F. Saurini, P. Lechat, L. Dandolo, M. Hamon, J. Mallet, G. Vodjdani, Disruption of the nonneuronal tph1 gene demonstrates the importance of peripheral serotonin in cardiac function. *Proc. Natl. Acad. Sci. U.S.A.* **100**, 13525–13530 (2003).
15. G. Sumara, O. Sumara, J. K. Kim, G. Karsenty, Gut-derived serotonin is a multifunctional determinant to fasting adaptation. *Cell Metab.* **16**, 588–600 (2012).
16. W. Choi, J. Namkung, I. Hwang, H. Kim, A. Lim, H. J. Park, H. W. Lee, K.-H. Han, S. Park, J.-S. Jeong, G. Bang, Y. H. Kim, V. K. Yadav, G. Karsenty, Y. S. Ju, C. Choi, J. M. Suh, J. Y. Park, S. Park, H. Kim, Serotonin signals through a gut-liver axis to regulate hepatic steatosis. *Nat. Commun.* **9**, 4824 (2018).
17. J. D. Crane, R. Palanivel, E. P. Mottillo, A. L. Bujak, H. Wang, R. J. Ford, A. Collins, R. M. Blümer, M. D. Fullerton, J. M. Yabut, J. J. Kim, J.-E. Ghia, S. M. Hamza, K. M. Morrison, J. D. Schertzer, J. R. B. Dyck, W. I. Khan, G. R. Steinberg, Inhibiting peripheral serotonin synthesis reduces obesity and metabolic dysfunction by promoting brown adipose tissue thermogenesis. *Nat. Med.* **21**, 166–172 (2015).
18. C.-M. Oh, J. Namkung, Y. Go, K. E. Shong, K. Kim, H. Kim, B.-Y. Park, H. W. Lee, Y. H. Jeon, J. Song, M. Shong, V. K. Yadav, G. Karsenty, S. Kajimura, I.-K. Lee, S. Park, H. Kim, Regulation of systemic energy homeostasis by serotonin in adipose tissues. *Nat. Commun.* **6**, 6794 (2015).
19. Y. Chabbi-Achengli, A. E. Coudert, J. Callebert, V. Geoffroy, F. Côté, C. Collet, M.-C. de Vernejoul, Decreased osteoclastogenesis in serotonin-deficient mice. *Proc. Natl. Acad. Sci. U.S.A.* **109**, 2567–2572 (2012).
20. H. Kim, Y. Toyofuku, F. C. Lynn, E. Chak, T. Uchida, H. Mizukami, Y. Fujitani, R. Kawamori, T. Miyatsuka, Y. Kosaka, K. Yang, G. Honig, M. van der Hart, N. Kishimoto, J. Wang, S. Yagihashi, L. H. Tecott, H. Watada, M. S. German, Serotonin regulates pancreatic beta cell mass during pregnancy. *Nat. Med.* **16**, 804–808 (2010).
21. M. Ohara-Imaizumi, H. Kim, M. Yoshida, T. Fujiwara, K. Aoyagi, Y. Toyofuku, Y. Nakamichi, C. Nishiwaki, T. Okamura, T. Uchida, Y. Fujitani, K. Akagawa, M. Kakei, H. Watada, M. S. German, S. Nagamatsu, Serotonin regulates glucose-stimulated insulin secretion from pancreatic β cells during pregnancy. *Proc. Natl. Acad. Sci. U.S.A.* **110**, 19420–19425 (2013).
22. J. H. Moon, Y. G. Kim, K. Kim, S. Osonoi, S. Wang, D. C. Saunders, J. Wang, K. Yang, H. Kim, J. Lee, J.-S. Jeong, R. R. Banerjee, S. K. Kim, Y. Wu, H. Mizukami, A. C. Powers, M. S. German, H. Kim, Serotonin regulates adult β-cell mass by stimulating perinatal β-cell proliferation. *Diabetes* **69**, 205–214 (2020).
23. C. Huang, F. Snider, J. C. Cross, Prolactin receptor is required for normal glucose homeostasis and modulation of β-cell mass during pregnancy. *Endocrinology* **150**, 1618–1626 (2009).
24. R. R. Banerjee, H. A. Cyphert, E. M. Walker, H. Chakravarthy, H. Peiris, X. Gu, Y. Liu, E. Conrad, L. Goodrich, R. W. Stein, S. K. Kim, Gestational diabetes mellitus from inactivation of prolactin receptor and MafB in islet β-cells. *Diabetes* **65**, 2331–2341 (2016).
25. A. E. Butler, J. Janson, S. Bonner-Weir, R. Ritzel, R. A. Rizza, P. C. Butler, β-cell deficit and increased β-cell apoptosis in humans with type 2 diabetes. *Diabetes* **52**, 102–110 (2003).
26. C. Chen, C. M. Cohrs, J. Stertmann, R. Bozsak, S. Speier, Human beta cell mass and function in diabetes: Recent advances in knowledge and technologies to understand disease pathogenesis. *Mol. Metab.* **6**, 943–957 (2017).
27. A. Schraenen, K. Lemaire, G. de Faudeur, N. Hendrickx, M. Granvik, L. Van Lommel, J. Mallet, G. Vodjdani, P. Gilon, N. Binart, P. in't Veld, F. Schuit, Placental lactogens induce serotonin biosynthesis in a subset of mouse beta cells during pregnancy. *Diabetologia* **53**, 2589–2599 (2010).
28. H. Bennet, I. G. Mollet, A. Balhuizen, A. Medina, C. Nagorny, A. Bagge, J. Fadista, E. Ottosson-Laakso, P. Vikman, M. Dekker-Nitert, L. Eliasson, N. Wierup, I. Artner, M. Fex, Serotonin (5-HT) receptor 2b activation augments glucose-stimulated insulin secretion in human and mouse islets of Langerhans. *Diabetologia* **59**, 744–754 (2016).
29. M. S. Estevao, L. C. Carvalho, D. Ribeiro, D. Couto, M. Freitas, A. Gomes, L. M. Ferreira, E. Fernandes, M. M. B. Marques, Antioxidant activity of unexplored indole derivatives: Synthesis and screening. *Eur. J. Med. Chem.* **45**, 4869–4878 (2010).
30. H. Kim, H. Kim, K. Kim, M. S. German, H. Kim, Ectopic serotonin production in β-cell specific transgenic mice. *Biochem. Biophys. Res. Commun.* **495**, 1986–1991 (2018).
31. B. Brouwers, G. de Faudeur, A. B. Osipovich, L. Goyvaerts, K. Lemaire, L. Boesmans, E. J. G. Cauwelier, M. Granvik, V. P. E. G. Pruniau, L. Van Lommel, J. Van Schoors, J. S. Stancill, I. Smolders, V. Goffin, N. Binart, P. in't Veld, J. Declercq, M. A. Magnuson, J. W. M. Creemers, F. Schuit, A. Schraenen, Impaired islet function in commonly used transgenic mouse lines due to human growth hormone minigene expression. *Cell Metab.* **20**, 979–990 (2014).
32. A.-G. Ziegler, M. Wallner, I. Kaiser, M. Rossbauer, M. H. Harsunen, L. Lachmann, J. Maier, C. Winkler, S. Hummel, Long-term protective effect of lactation on the development of type 2 diabetes in women with recent gestational diabetes mellitus. *Diabetes* **61**, 3167–3171 (2012).
33. H. Bennet, A. Balhuizen, A. Medina, M. Dekker Nitert, E. Ottosson Laakso, S. Essén, P. Spégel, P. Storm, U. Krus, N. Wierup, M. Fex, Altered serotonin (5-HT) 1D and 2A receptor expression may contribute to defective insulin and glucagon secretion in human type 2 diabetes. *Peptides* **71**, 113–120 (2015).
34. J. Almaca, J. Molina, D. Menegaz, A. N. Pronin, A. Tamayo, V. Slepak, P.-O. Berggren, A. Caicedo, Human beta cells produce and release serotonin to inhibit glucagon secretion from alpha cells. *Cell Rep.* **17**, 3281–3291 (2016).
35. Y. G. Kim, J. H. Moon, K. Kim, H. Kim, J. Kim, J.-S. Jeong, J. Lee, S. Kang, J. S. Park, H. Kim, β-cell serotonin production is associated with female sex, old age, and diabetes-free condition. *Biochem. Biophys. Res. Commun.* **493**, 1197–1203 (2017).
36. A. Martin-Montalvo, L. López-Noriega, C. Jiménez-Moreno, A. Herranz, P. I. Lorenzo, N. Cobo-Vuilleumier, A. Tamayo, C. González-Guerrero, J. S. W. R. Hofsteede, F. Lebreton, D. Bosco, M. G. Toscano, L. Herranz, J. Anselmo, J. C. Moreno, B. R. Gauthier, Transient *PAX8* expression in islets during pregnancy correlates with β-cell survival, revealing a novel candidate gene in gestational diabetes mellitus. *Diabetes* **68**, 109–118 (2019).

37. R. Retnakaran, C. Ye, C. K. Kramer, P. W. Connelly, A. J. Hanley, M. Sermer, B. Zinman, Maternal serum prolactin and prediction of postpartum β-cell function and risk of prediabetes/diabetes. *Diabetes Care* **39**, 1250–1258 (2016).
38. S. Lenzen, J. Drinkgern, M. Tiedge, Low antioxidant enzyme gene expression in pancreatic islets compared with various other mouse tissues. *Free Radic. Biol. Med.* **20**, 463–466 (1996).
39. R. P. Robertson, J. S. Harmon, Pancreatic islet β-cell and oxidative stress: The importance of glutathione peroxidase. *FEBS Lett.* **581**, 3743–3748 (2007).
40. N. Hou, S. Torii, N. Saito, M. Hosaka, T. Takeuchi, Reactive oxygen species-mediated pancreatic β-cell death is regulated by interactions between stress-activated protein kinases, p38 and c-Jun N-terminal kinase, and mitogen-activated protein kinase phosphatases. *Endocrinology* **149**, 1654–1665 (2008).
41. H. Mizukami, K. Takahashi, W. Inaba, K. Tsuboi, S. Osonoi, T. Yoshida, S. Yagihashi, Involvement of oxidative stress–induced DNA damage, endoplasmic reticulum stress, and autophagy deficits in the decline of β-cell mass in Japanese type 2 diabetic patients. *Diabetes Care* **37**, 1966–1974 (2014).
42. I. Gülçin, Measurement of antioxidant ability of melatonin and serotonin by the DMPD and CUPRAC methods as trolox equivalent. *J. Enzyme Inhib. Med. Chem.* **23**, 871–876 (2008).
43. C. Cangiano, A. Laviano, M. Del Ben, I. Preziosa, F. Angelico, A. Cascino, F. Rossi-Fanelli, Effects of oral 5-hydroxy-tryptophan on energy intake and macronutrient selection in non-insulin dependent diabetic patients. *Int. J. Obes. Relat. Metab. Disord.* **22**, 648–654 (1998).
44. L. R. Cataldo Bascuñan, C. Lyons, H. Bennet, I. Artner, M. Fex, Serotonergic regulation of insulin secretion. *Acta Physiol (Oxf.)* **225**, e13101 (2019).
45. L. R. Cataldo, M. L. Mizgier, R. B. Sagua, F. Jaña, C. Cárdenas, P. Llanos, D. Busso, P. Olmos, J. E. Galgani, J. L. Santos, V. A. Cortés, Prolonged activation of the Htr2b serotonin receptor impairs glucose stimulated insulin secretion and mitochondrial function in MIN6 cells. *PLOS ONE* **12**, e0170213 (2017).
46. K. Kim, C.-M. Oh, M. Ohara-Imaizumi, S. Park, J. Namkung, V. K. Yadav, N. A. Tamarina, M. W. Roe, L. H. Philipson, G. Karsenty, S. Nagamatsu, M. S. German, H. Kim, Functional role of serotonin in insulin secretion in a diet-induced insulin-resistant state. *Endocrinology* **156**, 444–452 (2015).
47. B. E. Metzger, Summary and recommendations of the third international workshop-conference on gestational diabetes mellitus. *Diabetes* **40**, 197–201 (1991).
48. World Medical Association, *Declaration of Helsinki, 1989. Ethical Principles for Medical Research Involving Human Subjects* (World Medical Association, 2005).
49. M. Matsuda, R. A. DeFronzo, Insulin sensitivity indices obtained from oral glucose tolerance testing: Comparison with the euglycemic insulin clamp. *Diabetes Care* **22**, 1462–1470 (1999).
50. A. Tura, A. Kautzky-Willer, G. Pacini, Insulinogenic indices from insulin and C-peptide: Comparison of beta-cell function from OGTT and IVGTT. *Diabetes Res. Clin. Pract.* **72**, 298–301 (2006).
51. R. Retnakaran, Y. Qi, M. I. Goran, J. K. Hamilton, Evaluation of proposed oral disposition index measures in relation to the actual disposition index. *Diabet. Med.* **26**, 1198–1203 (2009).
52. G. Gu, J. Dubauskaite, D. A. Melton, Direct evidence for the pancreatic lineage: NGN3+ cells are islet progenitors and are distinct from duct progenitors. *Development* **129**, 2447–2457 (2002).
53. H. Kim, Y. G. Kim, W. Choi, J. H. Moon, I. Hwang, K. Kim, V. K. Yadav, G. Karsenty, J.-S. Jeong, H. Kim, Generation of a highly efficient and tissue-specific tryptophan hydroxylase 1 knockout mouse model. *Sci. Rep.* **8**, 17642 (2018).
54. P. L. Herrera, L. Orci, J. D. Vassalli, Two transgenic approaches to define the cell lineages in endocrine pancreas development. *Mol. Cell. Endocrinol.* **140**, 45–50 (1998).
55. P. L. Herrera, Adult insulin- and glucagon-producing cells differentiate from two independent cell lineages. *Development* **127**, 2317–2322 (2000).
56. V. K. Yadav, J.-H. Ryu, N. Suda, K. Tanaka, J. A. Gingrich, G. Schütz, F. H. Glorieux, C. Y. Chiang, J. D. Zajac, K. L. Insogna, J. J. Mann, R. Hen, P. Ducy, G. Karsenty, Lrp5 controls bone formation by inhibiting serotonin synthesis in the duodenum. *Cell* **135**, 825–837 (2008).
57. M. A. Magnuson, A. B. Osipovich, Pancreas-specific Cre driver lines and considerations for their prudent use. *Cell Metab.* **18**, 9–20 (2013).
58. S. Srinivas, T. Watanabe, C.-S. Lin, C. M. William, Y. Tanabe, T. M. Jessell, F. Costantini, Cre reporter strains produced by targeted insertion of *EYFP* and *ECFP* into the *ROSA26* locus. *BMC Dev. Biol.* **1**, 4 (2001).
59. Y. Liu, J. Suckale, J. Masjkur, M. G. Magro, A. Steffen, K. Anastassiadis, M. Solimena, Tamoxifen-independent recombination in the *RIP-CreER* mouse. *PLOS ONE* **5**, e13533 (2010).
60. G. L. Szot, P. Koudria, J. A. Bluestone, Murine pancreatic islet isolation. *J. Vis. Exp.*, 255 (2007).
61. N. E. Sanjana, O. Shalem, F. Zhang, Improved vectors and genome-wide libraries for CRISPR screening. *Nat. Methods* **11**, 783–784 (2014).
62. O. Shalem, N. E. Sanjana, E. Hartenian, X. Shi, D. A. Scott, T. S. Mikkelsen, D. Heckl, B. L. Ebert, D. E. Root, J. G. Doench, F. Zhang, Genome-scale CRISPR-Cas9 knockout screening in human cells. *Science* **343**, 84–87 (2014).
63. P. D. Hsu, D. A. Scott, J. A. Weinstein, F. A. Ran, S. Konermann, V. Agarwala, Y. Li, E. J. Fine, X. Wu, O. Shalem, T. J. Cradick, L. A. Marraffini, G. Bao, F. Zhang, DNA targeting specificity of RNA-guided Cas9 nucleases. *Nat. Biotechnol.* **31**, 827–832 (2013).
64. S. Bae, J. Park, J. S. Kim, Cas-OFFinder: A fast and versatile algorithm that searches for potential off-target sites of Cas9 RNA-guided endonucleases. *Bioinformatics* **30**, 1473–1475 (2014).
65. V. Fogliano, V. Verde, G. Randazzo, A. Ritieni, Method for measuring antioxidant activity and its application to monitoring the antioxidant capacity of wines. *J. Agric. Food Chem.* **47**, 1035–1040 (1999).

Acknowledgments: We would like to express deep gratitude to Professor Kap-Bum Huh, who devoted himself to the education of physician-scientists in Korea and passed away a while ago. We thank H.-S. Jung, J. E. Kim, H. N. Jung, and S.-I. Chang (Korea Advanced Institute of Science and Technology) for technical support; D. Jang for graphical support; G. Karsenty (Columbia University) for *Htr2b* floxed mice; and H. J. Kim (Korea Advanced Institute of Science and Technology) and all of the laboratory members for their helpful discussions. **Funding:** This work was supported by grants from the National Research Foundation (NRF) of Korea (grant numbers: NRF-2017H1A2A1042095 to J.H.M., NRF-2013H1A8A1003985 and NRF-2018R1A6A3A01012333 to Hyeongseok Kim, and NRF-2015M3A9B3028218 and NRF-2018R1A2A3074646 to Hail Kim); NIH (Mentored Clinical Scientist Development Award K08 to R.R.B., P30 DK116074-01, UC4 DK104211, and P30 DK116071 to S.K.K., and P30 DK063720 to M.S.G.); Larry L. Hillblom Foundation (2018-D-0006-NET) to M.S.G.; the National Research Council of Science & Technology (NST) of Korea (CRC-16-01-KRICT) to S.J.; support from the H.L. Snyder Foundation, Elser Trust, Howard Hughes Medical Institute, grants from the Juvenile Diabetes Research Foundation and Helmsley Trust, and a gift from Steven and Michele Kirsch to S.K.K.; and Health Fellowship Foundation to J.H.M. **Author contributions:** J.H.M., Hyeongseok Kim, M.S.G., H.C.J., and Hail Kim generated the hypothesis, designed the experiments, and wrote the manuscript. J.H.M., Hyeongseok Kim, Hyunki Kim, J.P., Wonsuk Choi, Wongun Choi, H.J.H., H.-J.R., S.J., and R.R.B. performed and analyzed the animal experiments. J.H.M., S.H.C., N.H.C., and H.C.J. performed and analyzed the human experiments. J.H.M., Hyeongseok Kim, M.S., S.K.K., M.S.G., H.C.J., and Hail Kim analyzed the data and reviewed the manuscript. **Competing interests:** The authors declare that they have no competing interests. **Data and materials availability:** All data associated with this study are present in the paper or the Supplementary Materials.

Submitted 15 May 2019
Resubmitted 23 December 2019
Accepted 4 March 2020
Published 29 April 2020
10.1126/scitranslmed.aay0455

Citation: J. H. Moon, H. Kim, H. Kim, J. Park, W. Choi, W. Choi, H. J. Hong, H.-J. Ro, S. Jun, S. H. Choi, R. R. Banerjee, M. Shong, N. H. Cho, S. K. Kim, M. S. German, H. C. Jang, H. Kim, Lactation improves pancreatic β cell mass and function through serotonin production. *Sci. Transl. Med.* **12**, eaay0455 (2020).

Science Translational Medicine

Lactation improves pancreatic β cell mass and function through serotonin production

Joon Ho Moon, Hyeongseok Kim, Hyunki Kim, Jungsun Park, Wonsuk Choi, Wongun Choi, Hyun Jung Hong, Hyun-Joo Ro, Sangmi Jun, Sung Hee Choi, Ronadip R. Banerjee, Minho Shong, Nam Han Cho, Seung K. Kim, Michael S. German, Hak Chul Jang and Hail Kim

Sci Transl Med **12**, eaay0455.
DOI: 10.1126/scitranslmed.aay0455

Feeding with benefits

In addition to providing health benefits for infants, breastfeeding has also been reported to offer metabolic benefits for mothers, but the underlying biology explaining this observation has remained elusive. By studying both human and murine mothers over time, Moon *et al*. identified long-term improvements in pancreatic β cell mass and function, as well as glucose tolerance, all associated with lactation. The authors linked the hormone prolactin to serotonin production and proliferation of the β cells, providing a mechanistic explanation for the beneficial effects of lactation.

Science Translational Medicine (ISSN 1946-6242) is published by the American Association for the Advancement of Science, 1200 New York Avenue NW, Washington, DC 20005. The title *Science Translational Medicine* is a registered trademark of AAAS.